

PAPER • OPEN ACCESS

## Effect of concentration areas in sensitive analysis of a hybrid solar Brayton cycle

To cite this article: F Moreno-Gamboa *et al* 2021 *J. Phys.: Conf. Ser.* **2073** 012013

View the [article online](#) for updates and enhancements.

You may also like

- [A global optimization method synthesizing heat transfer and thermodynamics for the power generation system with Brayton cycle](#)

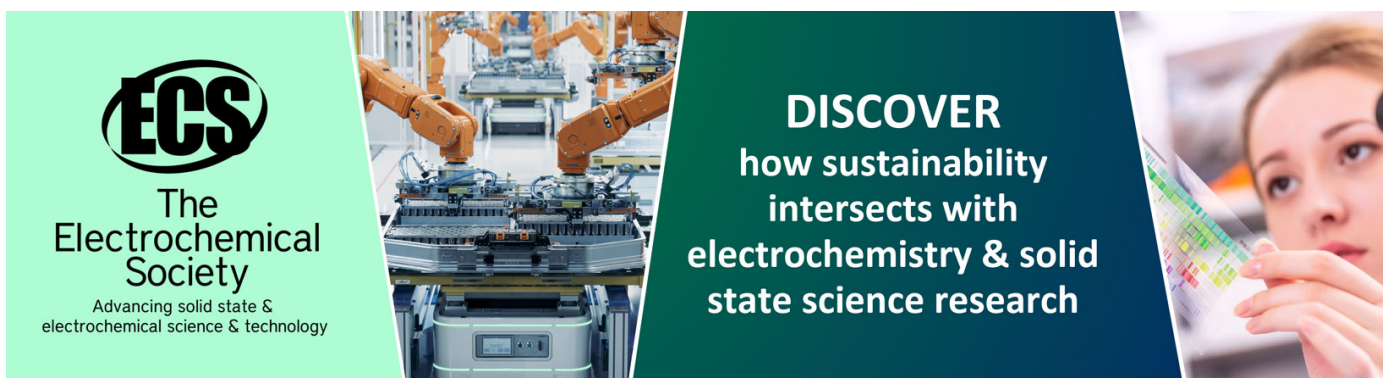
Rong-Huan Fu and Xing Zhang

- [Boosting thermodynamic performance by bending space-time](#)

Emily E. Ferketic and Sebastian Deffner

- [Influence of Supercritical Carbon Dioxide Brayton Cycle Parameters on Intelligent Circulation System and Its Optimization Strategy](#)

Kai Li and Kai Sun



**ECS**  
The  
Electrochemical  
Society  
Advancing solid state &  
electrochemical science & technology

**DISCOVER**  
how sustainability  
intersects with  
electrochemistry & solid  
state science research

# Effect of concentration areas in sensitive analysis of a hybrid solar Brayton cycle

F Moreno-Gamboa<sup>1</sup>, E Florez-Solano<sup>2</sup>, and E Espinel-Blanco<sup>2</sup>

<sup>1</sup> Grupo de Investigación en Fluidos y Térmicas, Universidad Francisco de Paula Santander, San José de Cúcuta, Colombia

<sup>2</sup> Grupo de Investigación en Tecnología y Desarrollo en Ingeniería, Universidad Francisco de Paula Santander, Seccional Ocaña, Colombia

E-mail: faustinomoreno@ufps.edu.co, eeespinelb@ufps.edu.co

**Abstract.** A simple hybrid solar thermal Brayton cycle plant thermodynamic model is evaluated in northern Colombia, where the maximum solar radiation values in the country are found. The model considers the different irreversibilities of the cycle and is coupled to a model for estimating direct solar radiation as a complementary energy source for the plant. The stability in the operation of the cycle is determined by a combustion chamber that complements the energy supply. As a result of the analysis, this work presents the sensitivity analysis of different operating parameters of the plant as a function of the areas of the concentration ratio of the solar system when the contribution of this system is maximum. It is observed that fuel consumption is reduced by 34.7% when increasing the concentration ratio between 200 and 700.

## 1. Introduction

The structure of the current energy markets must reduce polluting emissions and find alternative energy sources. In Colombia, 69% of electrical energy is produced from hydraulic systems, 29% from thermal plants that operate with coal and natural gas, and only 0.3% from renewable sources [1].

In the above scenario, there is a great expectation in concentrated solar power (CSP) systems [2]. A developing application focuses on the coupling of CSP systems with gas turbines, which can operate in different configurations and power ranges, making them very versatile in terms of location and type of application [3]. The solar resource is not constant, which presents a challenge that can be solved with hybridization using a combustor that ensures the turbine inlet temperature, even when the solar resource is not available [4]. Hybrid gas turbine systems with heliostat field solar concentrator and central tower are not commercially available except for small models of up to 100 kW [5], although experimental systems at Investigation and development confirm that the technology is technically feasible [6]. As any developing technology, hybrid CSP systems with gas turbine require important works in the coupling and control of the hybrid heat supply system with the power cycle and the solar receiver [7].

Considering that the northern region of Colombia has the potential for the development of CSP systems [8]. This paper presents a model for the estimation of direct solar radiation, coupled to a thermodynamic model of a hybrid Brayton cycle solar thermal plant. From the variation of the area of the heliostat field and the area of the receiver of the central tower, the influence of the concentration ratio in different parameters of the plant is evaluated, when the solar radiation is maximum around the solar noon.



## 2. Solar hybrid thermal power plant and models

This section describes the Brayton cycle hybrid solar plant, the solar resource estimation model, and the thermodynamic model of the plant.

### 2.1. Overall plant model

The analysis of the hybrid Brayton cycle solar power plant carried out in this work is based in the schematic in Figure 1. In this, the configuration of a hybrid Brayton cycle concentrating solar power plant is shown in Figure 1(a) and the temperature vs. entropy diagram as see Figure 1(b). The plant is composed of a compressor-turbine. At the compressor outlet, the heat supply begins, starting with the regenerator (process 2-x). Subsequently, the solar receiver (process x-y) receives the concentrated irradiation from the heliostat field. The last heat supply process is a combustion chamber (process y-5). After the regenerator, heat is dissipated to the environment by a heat exchanger (process 1-z).

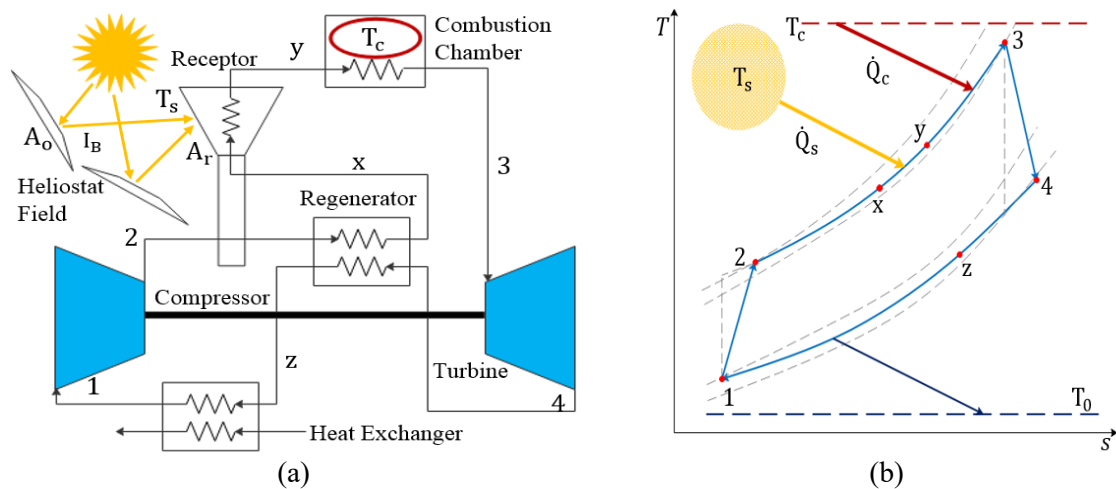


**Figure 1.** (a) scheme of the hybrid solar Brayton power plant; (b) temperature-entropy diagram.

### 2.2. Solar and optical model

Because of its operating conditions, a concentrating solar power system requires direct solar radiation ( $I_{DNI}$ ) at some location. Therefore, long-term measurements should be reliable. However, in many places in countries such as Colombia these data are not available, but they can be estimated with theoretical models, such as the one developed by Gueymard [9], called daily integration (DI) model. The DI model, the total irradiance on a horizontal surface  $I_H$ , is defined as the sum of its components, the direct  $I_{DNI}$  and diffuse  $I_{DH}$  radiation; therefore, the direct radiation is defined in the Equation (1) [9].

$$I_{DNI} = I_H - I_{DH}. \quad (1)$$

In order to distribute the radiation values over the day, the hour to day relationships for diffuse  $r_d$  and global  $r_t$  radiation is introduced in the Equation (1) y Equation (2) [9].

$$r_d = I_{DH} / \bar{D}_H, \quad (2)$$

$$r_t = I_H / \bar{H}_H, \quad (3)$$

where  $\bar{D}_h$  and  $\bar{H}_h$  represent the long-term monthly mean daily value for total and diffuse radiation, which are found at the National Aeronautics and Space Administration website. Direct radiation as a function of time-of-day ratios and global and diffuse radiation is expressed in the Equation (4) [9].

$$I_{DNI} = r_t \bar{H}_H - r_d \bar{D}_H, \quad (4)$$

The efficiency of the solar concentration power system ( $\eta_s$ ) (see Equation (5)) [4], can be defined as a function of the optical efficiency ( $\eta_0$ ), the losses in the central receiver by conduction and convection ( $U_1$ ), in the first term of Equation (5) and the losses by radiation which are the last term effective emissivity ( $\alpha$ ) and Stefan–Boltzmann constant ( $\sigma$ ). In addition, the concentration area ratio (Heliostat field area/receptor area ( $A_o/A_r$ )) and the ambient ( $T_0$ ) and receiver ( $T_s$ ) temperatures are included.

$$\eta_s = \eta_0 - \frac{U_1(T_s - T_0)}{((I_{DNI})(A_o/A_r))} - \frac{\alpha\sigma(T_s^4 - T_0^4)}{((I_{DNI})(A_o/A_r))}. \quad (5)$$

### 2.3. Power unit model

According to Figure 1, a regenerative Brayton cycle is considered, with the irreversibility as shown in the T-s diagram in the Figure 1(b). The complete thermodynamic model was previously detailed and validated by our research group for central tower plants [10]. The total heat supplied to the power cycle ( $\dot{Q}_h$ ) equals the sum of  $\dot{Q}_s$  and  $\dot{Q}_c$  which represent the external heat supplied to the working fluid by the solar concentrating system and the combustion chamber respectively. These can be presented as a function of the mass flow rate of the working fluid ( $\dot{m}$ ) and the enthalpies ( $h$ ) as show in the Equation (6) [10].

$$\dot{Q}_h = \dot{Q}_c + \dot{Q}_s = \dot{m}(h_3 - h_y) + \dot{m}(h_y - h_x) = \dot{m}(h_3 - h_x). \quad (6)$$

The definition of the heat input makes it possible to determine the solar factor ( $f$ ), which is the fraction of the solar heat received by the working fluid, expressed as the Equation (7) [10].

$$f = \dot{Q}_s / \dot{Q}_h = \dot{Q}_s / (\dot{Q}_c + \dot{Q}_s). \quad (7)$$

The solar thermal power plant output,  $P$  is evaluated in the Equation (8) [10].

$$P = \dot{m}(h_3 - h_4) + \dot{m}(h_2 - h_1). \quad (8)$$

Whit the Equation (9) [10] it is possible to determine power cycle performance is ( $\eta_h = P/\dot{Q}_h$ ) and the overall performance ( $\eta$ ) of the plant.

$$\eta = P / (\dot{m}_f Q_{lhv} + I_B A_o). \quad (9)$$

Fuel consumption can be estimated from the heat supplied by the combustion chamber, the efficiency of the chamber ( $\eta_{cc}$ ), the effectiveness of its heat exchanger ( $\epsilon_{ic}$ ) and the lower heating value ( $Q_{lhv}$ ) using the Equation (10) [10].

$$\dot{m}_f = \dot{m}(h_3 - h_y) / \eta_{cc} \epsilon_{ic} Q_{lhv}, \quad (10)$$

Finally, the fuel conversion rate ( $r_e$ ) of the plant is defined as the power generated over the fuel energy consumed as show the Equation (11) [4].

$$r_e = P / (\dot{m}_f Q_{lhv}). \quad (11)$$

## 3. Result and discussion

This section presents the details of the model validation and the results of the sensitivity analysis. In the validation of the DI model in the city of Seville, Spain, for a day that is equivalent to July 20 and taking data from Meteosevilla website, which have been compared with those estimated by the model through mean absolute bias error (MABE) and root mean square error (RMSE), solar resource model

assessments are performed. For the DI model the value  $MABE=0.201085$  is within the range of 0 to 0.212 and for  $RMSE=0.226616$  is within the range of 0 to 0.329 both ranges taken from Yao, *et al.* [11].

The validation of the thermodynamic model is performed by comparing the results with the references [4,12]. The Table 1 shows the results of the validation of the thermodynamic model, where it can be observed that the maximum deviation is 1.28% corresponding to the power cycle efficiency ( $\eta_h$ ), which determines a very good fit of the model used. The details of the model and validation parameters can be found in detail in Moreno-Gamboa, *et al.* [10].

**Table 1.** Thermodynamic model assessment.

	P (kW)	$\eta_h$	$\eta$	f	$\dot{m}_f$ (kg/s)
Estimated model	4615.15	0.385	0.302	0.338	0.170
Reference [4,12]	4600	0.39	0.300	0.341	0.172
Deviation %	0.328	1.28	0.66	0.88	1.16

The Figure 2(a) shows the power (P) and ambient temperature [13], with reverse behaviors and relative amplitude of the power output is 3% throughout the day. The Figure 2(b) shows the hourly evolution of the solar factor, which shows a maximum value around noon (12 m) with a value  $f_{max} = 0.2546$ , coinciding with the solar noon for the city according to Global Monitoring Laboratory (ESRL) website. At this time of the day the energy supply by the combustion chamber is reduced to a minimum and is replaced by the energy supplied by the solar concentration system, while in the evening hours the solar factor is  $f = 0$ . In addition, Figure 2(b) shows the evolution of the overall efficiency of the plant, which decreases with the solar factor, due to the losses of the solar concentration system, showing a maximum reduction of 18.22% around midday with respect to the night.

The concentration ratio is defined as the ratio between the area of the heliostat field and the area of the central tower receiver ( $A_0/A_r$ ). This is the type of system where the concentration ratio can achieve the widest range of application (100 to 1500) [2]. Considering the importance of the concentrator areas in the operation of the system, this section evaluates the sensitivity of different operating parameters of the plant with respect to the heliostat field and central tower receiver areas when the solar fraction is maximum around noon as see in the Figure 2(b). This type of analysis is important when evaluating designs and deciding on the investment to be made in the plant or in some of its components.

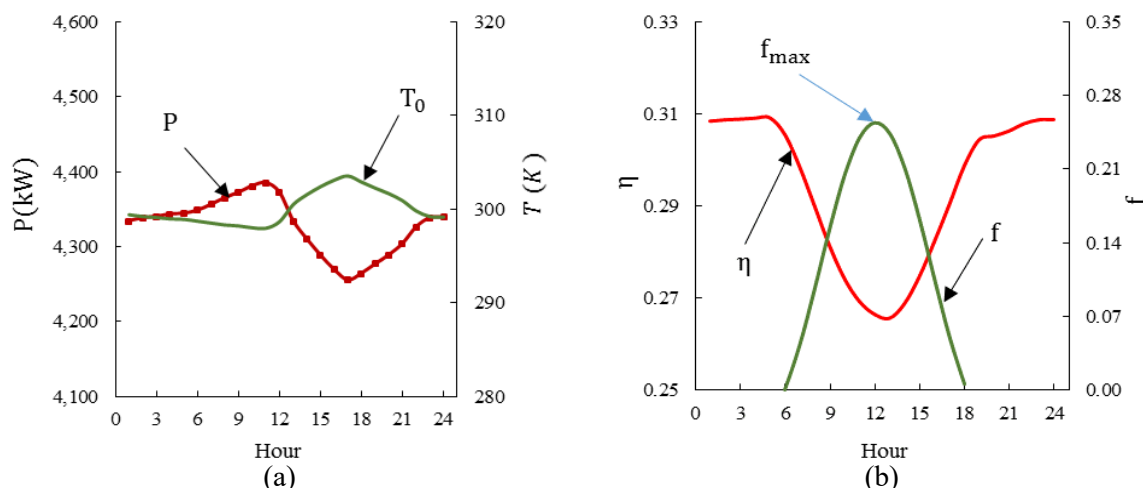


**Figure 2.** (a) power and ambient temperature; (b) evolution of overall efficiency and solar fraction.

To analyze the sensitivity of plant parameters with respect to the areas ( $A_0$ ,  $A_r$ ), typical figures of thermoeconomic analysis will be used useful in design processes. Figure 3 shows the evolution of the overall efficiency as a function of the variation of the areas ( $A_0$ ,  $A_r$ ) maintaining a constant at a time and represented on the horizontal axis the concentration ratio ( $A_0/A_r$ ), which is evaluated in a range

between 200 and 700 (Solugas plant value ( $A_o/A_r$ )=425.2 [14]). A variation between -52% and +64% can be observed in the real value defined the operating point (PO), in the range of the evaluated concentration relationship. Figure 3 shows, that the variation of  $\eta$  (for  $f_{\max}$ ) with respect to  $A_o$  is almost linear,  $\eta$  increases when the area of the heliostat field decreases due to increased energy losses that generates the optical efficiency. The overall efficiency decreases 14.3% in the evaluated range. On the other hand, increasing  $A_r$  shows a variation of only 1.8% increment in the overall efficiency, since this is the area with the smallest concentration size, producing a less linear variation, especially at low concentration ratios.

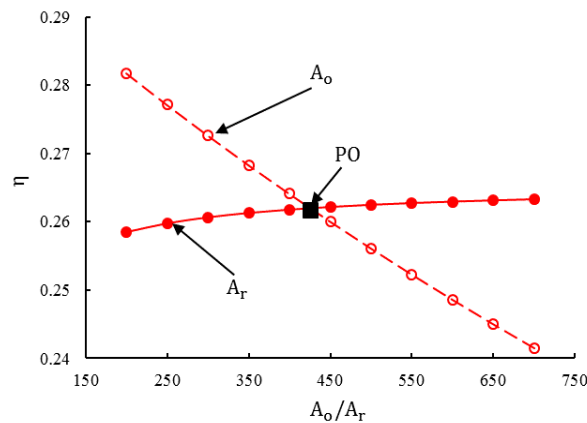


**Figure 3.** Sensitivity of the overall efficiency to changes in the concentration ratio in  $f_{\max}$ .

The concentration ratio has an important impact on the solar fraction, as shown in Figure 4(a), where  $f_{\max}$  increases by 260% with respect to the increase of ( $A_o/A_r$ ) in the evaluated range when  $A_o$  is increased. This is because the larger the heliostat field area, the more solar radiation is received by the system and the more energy is supplied to the power cycle. On the other hand, the increase of  $A_r$  only allows an increase of 8.4% in the maximum solar fraction. The increase of the solar factor determines the reduction of fuel consumption by reducing the energy requirement of the power cycle to the combustion chamber. Figure 4(b) shows the fuel consumption behavior of the system for  $f_{\max}$  inverse to the behavior of the solar factor, where it is observed that by increasing  $A_o$  in the evaluated range the fuel consumption reduction is 65.2%. Additionally, by increasing  $A_r$  the decrease in fuel consumption is only 2.6%.

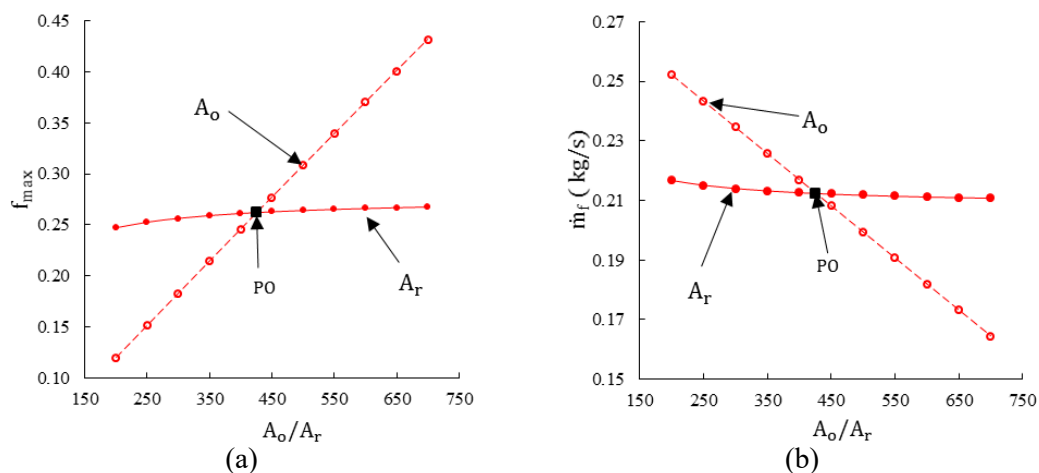


**Figure 4.** Sensitivity of the solar factor (a) and fuel consumption (b) to changes in the concentration ratio in  $f_{\max}$ .

An important parameter in the operation of the concentrating solar system is the central tower receiver temperature. Figure 5(a) shows the variation of the receiver temperature ( $T_s$ ) in  $f_{max}$  with respect to the concentration ratio given the higher power flux and it is observed that with the increase of  $A_o$  the increase of  $T_s$  is 23.6%, while with the increase of  $A_r$  the temperature increase is only 1.4%. Finally, the efficiency of the solar concentrator ( $\eta_s$ ) increases with the concentration ratio, as shown in Figure 5(b). The variation of  $\eta_s$  is strongly affected by the radiative heat losses of the receiver as see in the Equation (5), which are not linear. Additionally, increasing  $A_r$  generates an increase of  $\eta_s$  by 8.4% and increasing  $A_o$  produces an increase of  $\eta_s$  by 3.9%.

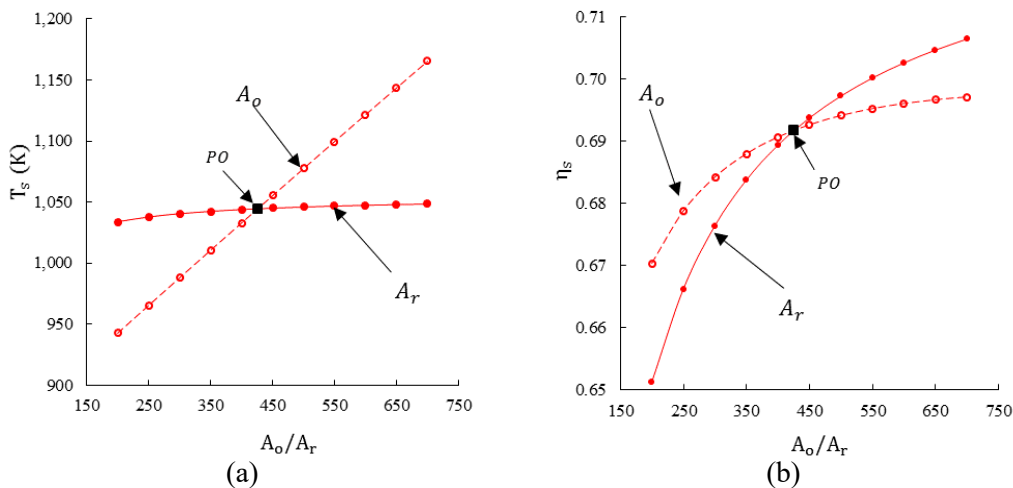


**Figure 5.** Sensitivity of central tower receiver operating temperature (a) and sensitive concentrator efficiency (b) to concentration ratio changes in  $f_{max}$ .

#### 4. Conclusions

The models presented can evaluate important plant parameters and by including the estimation of the solar resource by daily integration model allows applying the evaluation of the system in different locations and days of the year.

The models presented can evaluate important plant parameters and by including the estimation of the solar resource by daily integration model allows applying the evaluation of the system in different locations and days of the year. The area of the heliostat field affects the system because increasing this parameter also increases the possibility of receiving radiation and delivering energy to the cycle to reduce fuel consumption but affects the overall efficiency due to the losses generated by the optical efficiency, which in this case was assumed to be constant ( $\eta_0 = 0.73$ ). However, an optimization study of the size and distribution of the heliostat field according to the location of the plant is required.

Although solar receivers are still a developing technology, the effective receiving area especially affects the efficiency of the concentrator due to conduction, radiation and convection losses given the high operating temperature of the receiver, in the other parameters evaluated effective receiving area has a low influence on the variation of the same, however it does not allow such a linear variation.

#### References

- [1] Unidad de Planeación Minero-Energética (UPME) 2020 *Proyección de Demanda de Energía Eléctrica y Potencia Máxima en Colombia, Revisión Julio 2019* (Bogotá: Unidad de Planeación Minero-Energética)
- [2] Foster R, Ghassemi M, Cota A 2009 *Solar Energy. Renewable Energy and Environment* (Boca Raton: CRC Press)
- [3] Jamel M S, Rahman A, Shamsuddin A H 2013 Advances in the integration of solar thermal energy with conventional and non-conventional power plants *Renewable Sustainable Energy Reviews* **20** 71
- [4] Santos M J, Merchán R P, Medina A, Calvo Hernandez A 2016 Seasonal thermodynamic prediction of the performance of a hybrid solar gas-turbine power plant *Energy Conversion and Management* **115** 89

- [5] Doron P 2020 A high temperature receiver for a solarized micro-gas-turbine *AIP Conference Proceedings* **2303(1)** 030012
- [6] Dunham M T, Iverson B D 2014 High-efficiency thermodynamic power cycles for concentrated solar power systems *Renewable and Sustainable Energy Reviews* **30** 758
- [7] Olivenza-León D, Medina A, Calvo A 2016 Thermodynamic modeling of a hybrid solar gas-turbine power plant *Energy Conversion and Management* **93** 435
- [8] Guzman L, Henao A, Vasquez R 2014 Simulation and optimization of a parabolic trough solar power plant in the city of Barranquilla by using system advisor model (SAM) *Energy Procedia* **57** 497
- [9] Gueymard C A 2000 Prediction and performance assessment of mean hourly global radiation *Solar Energy* **68(3)** 285
- [10] Moreno F, Escudero A, Nieto C 2020 Performance evaluation of external fired hybrid solar gas-turbine power plant in Colombia using energy and exergy methods *Thermal Science and Engineering Progress* **20** 100679
- [11] Yao W, Li Z, Xiu T, Lu Y, Li X 2015 New decomposition models to estimate hourly global solar radiation from the daily value *Solar Energy* **120** 87
- [12] Merchan R P, Santos M J, Medina A, Calvo Hernandez A 2018 Thermodynamic model of a hybrid Brayton thermosolar plant *Renewable Energy* **128** 473
- [13] Ramírez E, Acosta M, Vélez J 2017 Análisis de condiciones climatológicas de precipitaciones de corto plazo en zonas urbanas: caso de estudio Barranquilla, Colombia *Idesia* **35(2)** 87
- [14] Merchán R, Santos M, Heras I, Gonzalez J, Medina A, Calvo A 2020 On-design pre-optimization and off-design analysis of hybrid Brayton thermosolar tower power plants for different fluids and plant configurations *Renewable and Sustainable Energy Reviews* **119** 109590